Plants-Derived Fluorescent Silicon Nanoparticles Featuring Excitation Wavelength-Dependent Fluorescent Spectra for Anti-Counterfeiting Application

Yanyan Wu‡, Yiling Zhong‡, Binbin Chu, Bin Sun, Bin Song, Sicong Wu, Yuanyuan Su and Yao He*

Jiangsu Key Laboratory for Carbon-Based Functional Materials and Devices, Institute of Functional Nano and Soft Materials (FUNSOM), Soochow University, Suzhou 215123, China
E-mail: yaohe@suda.edu.cn

Supporting Information

Table of Contents

1. Materials and Devices ……..…….....S-3

2. Methods…….....S-5

3. Optical image of the amorphous silica prepared from rice husks. EDS pattern of the amorphous silica…….....S-8

4. Gram-scale fabrication of SiNPs prepared from RHA……....S-9

5. UV-PL spectra of SiNPs prepared from RHA…….……....S-10

6. TGA profiles of RH, RHA, C-dots, R-SiNPs, silicon wafer and a mixture of R-SiNPs and C-dots. Raman spectrums of RHA, SiNPs prepared from RHA and C-dots……...S-11

7. HRTEM, TEM image and DLS of the SiNPs.....S-13

8. ICP-OES analysis results…….……...….S-15

9. The XPS spectrum of the prepared SiNPs and RHA……...……S-16

10. FTIR spectra of SiNPs and RHA, as well as high-resolution XPS spectra of C 1s for SiNPs...…….S-17

10. Excitation-wavelengths-dependent emission spectra of SiNPs prepared from sugarcane bagasse. Temporal PL spectra and corresponding PL intensity of the SiNPs during 45-day storage in ambient environment are also presented…….……..….S-18
11. Excitation-wavelengths-dependent emission spectra of SiNPs prepared from wheat straws. Temporal PL spectra and corresponding PL intensity of the SiNPs during 40-day storage in ambient environment are also presented……...…S-19
13. Cytotoxicity assessment of R-SiNPs……...……S-20
14. References.....S-21

Materials and Devices. Hydrochloric acid (37 wt%), sodium hydroxide and citric acid were purchased from Sinopharm Chemical Reagent Co., Ltd. (China). Urea and rhodamine-6G were purchased from Sigma-Aldrich. All chemicals were used as received. All solutions were prepared using Milli-Q water (Millipore) as the solvent. The wheat straws, rice husks and sugarcanes were purchased from local markets. Phosphate-doped silicon (100) wafers were purchased from Heifei Kejing Materials Technology Co., Ltd. (China). The microwave system NOVA used for synthesizing silicon nanoparticles (SiNPs) was made by Preekem of Shanghai, China. The system operates at 2450 MHz frequency and works at 0-500 W power. Exclusive vitreous vessels with a volume of 15 or 20 mL are equipped for the system to provide security during reaction demanding high temperature and pressure. The SiNPs were characterized by UV-vis absorption, photoluminescence (PL), thermogravimetric analysis (TGA), Raman microscope, transmission electronic microscopy (TEM), high-resolution TEM (HRTEM), energy dispersive spectroscopy (EDS), powder X-ray diffraction (XRD), high-resolution X-ray photoelectron spectroscopy (XPS), inductively coupled plasma optical emission spectroscopy (ICP-OES). DynaPro dynamic light scatterer (DLS) and Fourier-transform infrared (FTIR) spectroscopy, Laser-scanning confocal fluorescent (Leica, TCS-SP5). PL measurements were performed using a HORIBA JOBIN YVON FLUOROMAX-4 spectrofluorimeter. The PLQY of samples was estimated using quinine sulfate in 0.1 M H_2SO_4 (literature quantum yield: 58%) as a reference standard, which was freshly prepared to reduce the measurement error.[1] TGA analysis was performed on a METTLER TOLEDO TGA/STDA 851 instrument. The samples, which ranged in weight from 5 to 12 mg, were placed in a porcelain crucible and heated under air atmosphere from 30 to 800 °C at a rate of 10 °C/min. TEM and HRTEM samples were prepared by dispersing the sample onto carbon-coated copper grids with the excess solvent evaporated. The TEM/HRTEM overview images were recorded using Philips CM 200 electron microscope operated at 200 kV. EDS spectroscopy was utilized to determine the fraction of the amorphous silica. The silica sample

was first dispersed onto a micro grid with the excess solvent evaporated. The sample was then characterized by using Philips CM 200 electron microscope, equipped with EDS spectroscopy. The XRD spectra were recorded on a Panalytical, Empyrean, X-ray diffractometer, operated at 40 mA and 40 kV. The SiNPs, rice husk ash, sugarcane bagasse ash and wheat straw ash were placed on a zero-background sample holder made of monocrystal silicon plate. After evaporating the SiNPs solvent, a film was formed and used for the measurement. A Raman microscope (HR800) equipped with a 633 nm He-Ne 20 mW laser (polarized 500:1) was employed for obtaining the Raman spectra. The acquisition and analysis of Raman data were performed by using the LabSpec5 software. Elemental analysis was conducted by inductively coupled plasma-optical emission spectroscopy (ICP-OES) using a Perkin-Elmer Optima DV8000 optical emission spectrometer. To exclude impurities in the SiNPs solution, such as sodium hydroxide in solution, the residual reagents were removed by dialysis (1 kDa). The solvent in the sample was adequately evaporated by vacuum drying for 8 h, producing the SiNPs solid powder. Then, the resultant sample was further resolved in 2 mL of HNO_3. The as-prepared SiNPs solution sample was transferred into a 50-mL flask, and diluted with purified water to volume for ICP-OES analysis. High-resolution X-ray photoelectron spectroscopy (XPS) analyses were performed using a Kratos AXIS Ultra^{DLD} ultrahigh vacuum (UHV) surface analysis system, which consists of a fast entry air lock (base pressure $< 1 \times 10^{-8}$ Torr), a multiport carousel chamber ($< 5 \times 10^{-10}$ Torr), a deposition chamber ($< 5 \times 10^{-10}$ Torr), and an analysis chamber ($< 3 \times 10^{-10}$ Torr). A monochromatic Al Kα source (1486.6 eV) with a resolution of 0.1 eV was used to irradiate the samples. XPS samples were prepared by drop-casting SiNPs (~2 mg) onto aluminum substrates and degassing at 10^{-7} Torr for 15 hours prior to analysis. For FTIR measurements, KBr was pressed into a slice, onto which the SiNPs sample was dropped. The solvent in the sample was adequately evaporated by irradiation (> 30 min) with a high-power incandescent lamp. FTIR spectra were recorded on a Bruker HYPERION FTIR spectrometer and cumulated 32 scans at a resolution of 4 cm^{-1}.

Light-scattering analysis was performed using a DLS, which was made by Malvern Corp, U.K. (ZEN3690). 1 mL SiNPs sample was transferred into an exclusive vitreous for DLS measurements. Experiment parameters were as follows: scan times: 100; dispersant: water; temperature: 25 ^{o}C; viscosity: 0.8872 cP; RI: 1.330; and dielectric constant: 78.5. Optical measurements were performed at room temperature under ambient air conditions. UV-vis absorption spectra were recorded with a Perkin-Elmer lambda 750 UV-vis near-infrared spectrophotometer. PL measurements were performed using a HORIBA JOBIN YVON FLUOROMAX-4 spectrofluorimeter. CRI (Cambridge Research Instrumentation) Maestro *in vivo* imaging system was utilized for imaging the stained paper, fingerprint and feather (excitation at 455 nm, emission at 475-515 nm, and exposure time 10000 ms; excitation at 523 nm, emission at 550-590 nm, and exposure time 10000 ms).

Methods

Microwave dielectric heating is utilized in our method to take advantage of its three dominant merits compared to conventional convective heating. First, sample temperature can be rapidly raised due to the high utilization factor of microwave energy, leading to high reaction rate. Second, thermal gradient effects can be effectively reduced due to the volumetric heating of microwaves, which is favorable for homogeneous heating and uniform product formation. Finally, reaction selectivity is improved under microwave irradiation (MWI) due to different dipole constants of various substances. Moreover, the microwave method can be readily scaled up to large reaction volumes. Consequently, the MWI methodology has been well demonstrated to be greatly facilitated reaction rates, selectivity and product yields, allowing rapid cleavage of large-size silicon materials to produce small-size nanoparticles.

Synthesis of SiNPs. The raw rice husks (RH), sugarcane bagasse (SB), and wheat straws (WS) were boiled in 10 wt % HCl solution for 3 h, rinsed with deionized water, and then dried at 60

°C for 24 h. The dried RH, SB, WS were then gently heated over an alcohol lamp (600-800 °C) to produce amorphous silica. 0.043 g ash were added to 10 mL 0.5 M NaOH to prepare the SiNPs precursor solution, and then transferred the resultant precursor solution into the exclusive vitreous vessel with a volume of 30 mL. The SiNPs were synthesized under reaction temperature and time of 160 °C and 120 min. After the reaction temperature cooled to smaller than 30 °C naturally, we removed the as-prepared SiNPs from the microwave oven.

In order to exclude impurities influence, such as sodium hydroxide in solution, dialysis (1 kDa) was used to remove the residual reagents. The purified SiNPs aqueous solution with strong luminescence was investigated for anti-counterfeiting applications and cytotoxicity assessment.

MTT assay of cell viability. Human breast adenocarcinoma cells (MCF-7 cells) were cultured in RPMI-1640 medium, supplemented with 10 % heat-inactivated fetal bovine serum (FBS) and antibiotics (100 μg/mL streptomycin and 100 U/mL penicillin) at 37 °C in the humidified atmosphere with 5% CO_2. The SiNPs solution whose concentration is the same as that used in the fluorescence imaging was added to each well (10 μl). Incubation was carried out for 3, 6, 12, 24, 48 h. The cytotoxicity of the SiNPs was evaluated by the MTT (3-(4, 5-dimethylthiazol-2-yl)-2, 5-diphenyltetrazolium bromide) assay (thiazolyl blue tetrazolium bromide (M5655)). The assay was based on the accumulation of dark-blue formazan crystals inside living cells after exposure to MTT, which is a well-established protocol for assessment of cellular viability.[2] Destruction of cell membranes by the addition of sodium dodecylsulfate resulted in the liberation and solubilization of crystals. The number of viable cells was thus directly proportional to the level of the initial formazan product created. The formazan concentration was finally quantified using a spectrophotometer by measuring the absorbance at 570 nm (ELISA reader). A linear relationship between cell number and optical density was

established, thus allowing for accurate quantification of changes in the rate of cell proliferation.

Fluorescence imaging by using the prepared SiNPs. A kind of commercial paper which featured no background fluorescence under the UV lamp was chosen. A butterfly pattern was designed and printed on commercially available paper, whose plumages were respectively dispersed with rhodamine-6G (R6G, left) and the SiNPs sample solution. The feather was coated with a drop of the aqueous solution of SiNPs and then dried under air. Before making the fingerprints, the hand of the fingerprint donor was washed in soap water sufficiently and air-dried. The sodium hydroxide in SiNPs solution was removed by dialysis (1 kDa), the cleaned finger gently wiped the purified SiNPs aqueous solution to prepare the fingerprint specimen. The stained paper, fingerprint and feather were examined by CRI Maestro *in vivo* imaging system with excitation at 455 nm, emission at 475-515 nm and 523 nm, emission at 550-590 nm.

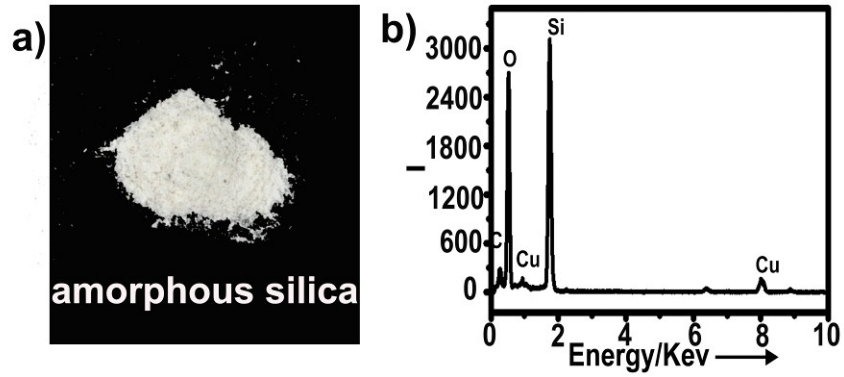

Fig. S1 (a) Optical image of the amorphous silica prepared from rice husks. (b) EDS pattern of the as-prepared amorphous silica. The EDS pattern reveals that the amorphous silica prepared from rice husks mainly contains Si and O, whereas a faint C peak located in ~0.27 Kev can be also observed, indicating a tiny amount of C is still existed in the silica sample. The reason is that rice husk has a fairly rigid structural backbone formed by silica to which the carbohydrates are bonded. As thus, a tiny amount of carbonous residues stay in the amorphous silica after pyrolysis. Similar results have been reported elsewhere,[3] consisted with our EDS results.

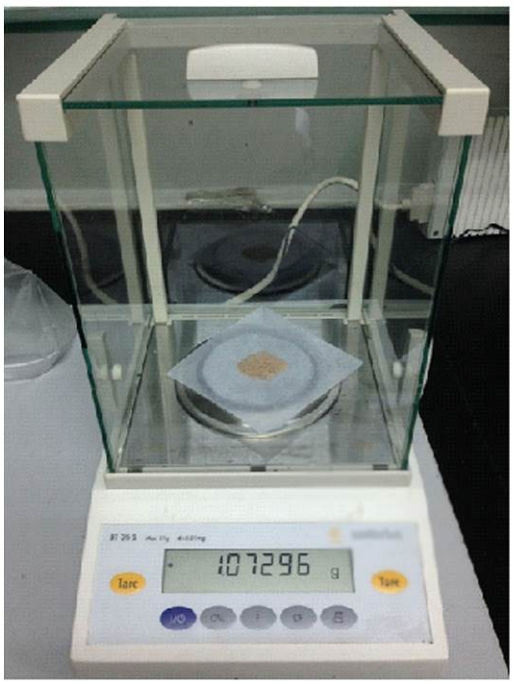

Fig. S2 Gram-scale fabrication of SiNPs from rice husks. The net weight of the product is shown on the screen of the balance. SiNPs can be derived directly from rice husks, an abundant agricultural byproduct produced at a rate of 1.2×10^8 tons/year,[4] with a conversion yield of 4.5% by mass.

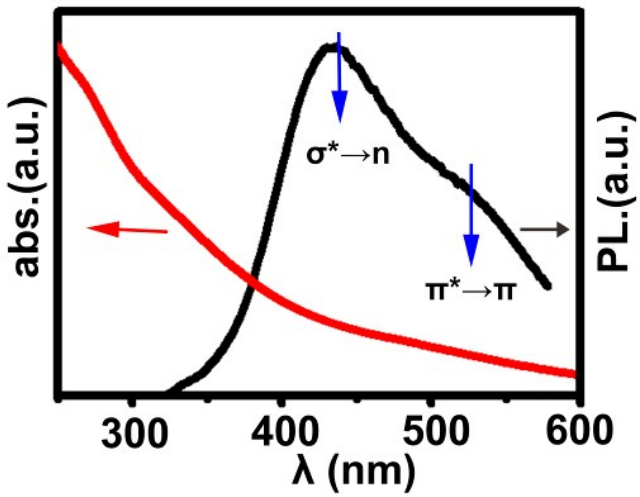

Fig. S3 Absorption and photoluminescence (UV-PL) spectra of the SiNPs prepared from rice husks. When excited at 300 nm, the SiNPs solution shows a peak at 440 nm and a shoulder at around 530 nm, which are ascribed to the σ*→n and π*→π transitions.[5]

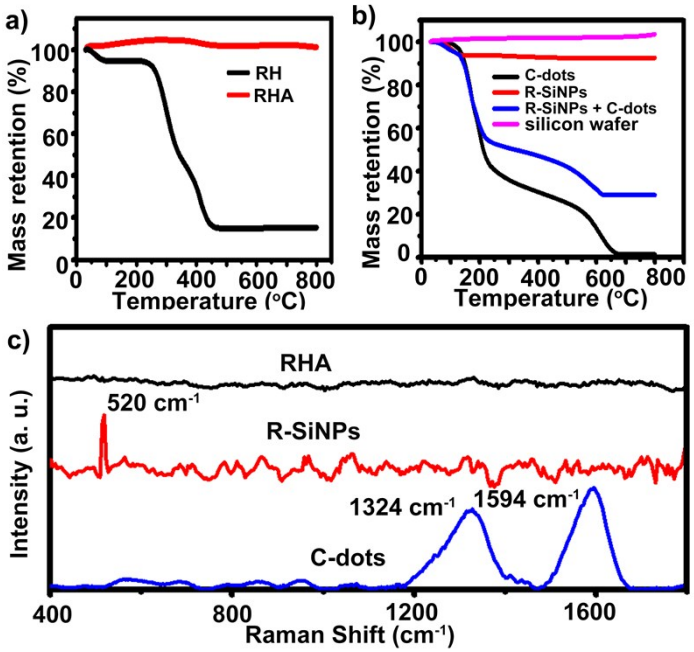

Fig. S4 (a) TGA profiles of RH (black line) and RHA (red line). (b) TGA profiles of C-dots (black line), R-SiNPs (red line), silicon wafer (pink line) and a mixture of R-SiNPs and C-dots (blue line, 5.160 g SiNPs, 10.489 g C-dots). The experiments are run at heating rate of 10 °C /min under air. (c) Raman spectrums of RHA (black line), SiNPs prepared from RHA (red line) and C-dots (blue line).

In order to study the weight loss/gain of the sample, thermogravimetric analysis (TGA) is carried out under a flow of air with an increase in temperature ranging from 30 °C to 800 °C. TGA of RH (Figure S4a, black line) shows a typical three-stage mass loss in air: (i) mass loss below 100 °C, which is attributed to water loss; (ii) mass loss around 300 °C, corresponding to cellulose/hemicellulose/lignin degradation; and (iii) mass loss between 350-500 °C, which is due to the burning of carbonous residues.[4] When an alcohol lamp with temperature about 600-800 °C is elected as the heat source, the raw RH are converted to silica by thermally decomposing the organic matter. Nearly no distinct increase or descrease of weight is observed in the TGA curve of the RHA sample (Figure S4a, red line) at a temperature range of 30 to 800 °C. The carbon-dots (C-dots) are used as a control group which are prepared based on previous reports.[6a] As shown in Figure S4b, in air, the C-dots undergo a catastrophic weight loss at temperatures > 200 °C.[6b] The organic is assumed to be fully disposed at the highest temperature, we thus can obtain the mass fraction of the organic component contained the SiNPs.[6c] The silicon wafers exhibit weight increase up to 800 °C, which is due to silicon

oxidation.[6d] Meanwhile, the mixture of C-dots and SiNPs materials (5.160 g SiNPs, 10.489 g C-dots) show rapid mass loss between 210 and 620 ^{o}C. In this temperature range, since the SiNPs powder are very stable during this temperature range, any weight change is thus corresponding to the oxidation of C-dots. The TGA profiles confirm the SiNPs do not contain C-dots, and the silica sample is relatively pure and accounts for as much as 10% of the dry weight of the rice husks. The Raman spectra further confirm the SiNPs do not contain C-dots. Typically, a peak at 520 cm^{-1} confirms the change of the amorphous silica form into crystalline silicon after reduction (Figure S4c, red line).[6e] In contrast, for the C-dots, their Raman spectra present two typical peaks locating at ~1324 cm^{-1} and 1594 cm^{-1}, resulted from the D band (sp3-hybridized) and G band (sp2-hybridized), respectively.[6a]

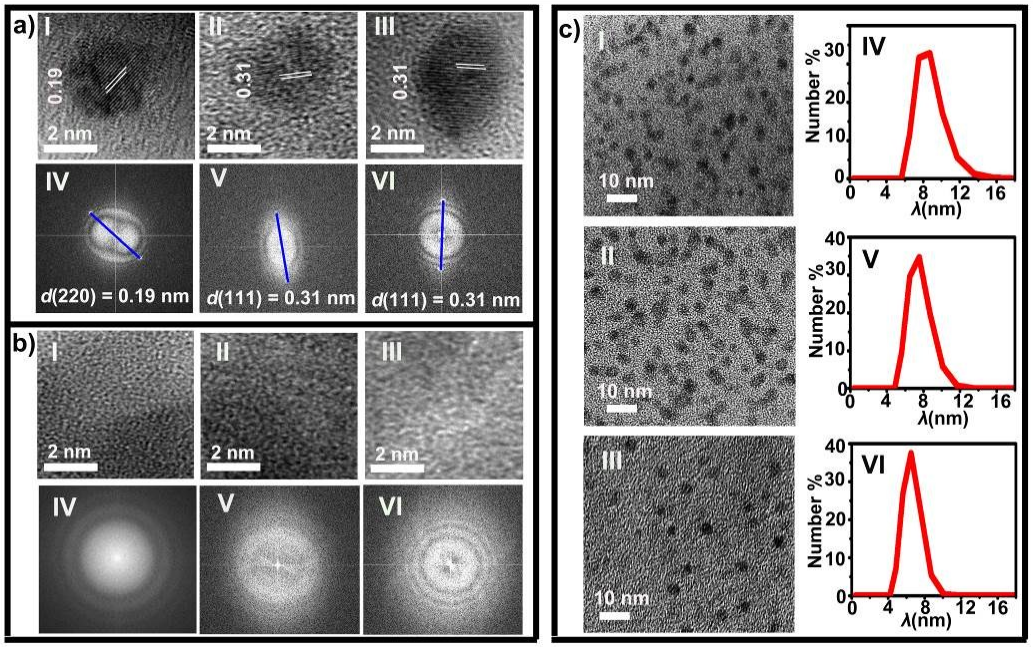

Fig. S5 (aI) HRTEM and (aIV) FFT images of the SiNPs prepared from rice husks. (aII) HRTEM and (aV) FFT images of the SiNPs prepared from sugarcane bagasse. (aIII) HRTEM and (aVI) FFT images of the SiNPs prepared from wheat straws. (bI) HRTEM and (bIV) FFT images of the silica sample prepared from rice husks. (bII) HRTEM and (bV) FFT images of the silica sample prepared from sugarcane bagasse. (bIII) HRTEM and (bVI) FFT images of the silica sample prepared from wheat straws. (cI) TEM image and (cIV) dynamic light scattering (DLS) of the SiNPs prepared from rice husks. (cII) TEM image and (cV) DLS of the SiNPs prepared from sugarcane bagasse. (cIII) TEM image and (cVI) DLS of the SiNPs prepared from wheat straws.

High-resolution transmission electron microscopy (HRTEM) characterization is employed for verifying the morphology and crystallinity of the resultant SiNPs. Typically, HRTEM images of the SiNPs presented in Figure S5a(I-III) show clear lattice fringes of SiNPs derived from all the three kinds of plants (i.e., RHA, SBA, and WSA), convincingly demonstrating high crystallinity of resultant SiNPs whose lattice plane correspond to the d-spacing of the cubic diamond structure of silicon giving the (220) plane with 0.19 nm spacing (Figure S5aI) or the (111) plane with 0.31 nm spacing (Figure S5aII and III). Corresponding fast Fourier transform (FFT) is also shown in Figure S5a(IV-VI), in which the set of spots with a lattice spacing of 0.19 nm or 0.31 nm can be indexed to the (220) or (111) reflection, respectively, indicating good crystallinity of the resultant SiNPs.[7a] In comparison, the control groups, *i.e.*, the amorphous silica extracted from rice husks, sugarcane bagasse, and wheat straws, do not show any crystallinity according to the HRTEM images (Figure S5b(I-III)), well consistent with the FFT analysis exhibiting diffused halo rings (Figure S5b(IV-VI)). As observed in the

transmission electron microscopy (TEM) images (Figure S5c(I-III)), the resultant SiNPs prepared from RHA (Figure S5cI), SBA (Figure S5cII) and WSA (Figure S5cIII) exhibit spherical structure, with an average diameter of ~4 nm and good monodispersibility. The diameter measured by dynamic light scattering (DLS) further confirms the small size of the as-prepared SiNPs with a hydrodynamic diameter ranging ~7-8 nm, as shown in Figure S5c (IV-VI). The distinct conditions for TEM and DLS characterizations leads to slight difference of the diameters determined using TEM and DLS. Briefly, in case of TEM measurement, the solvent is required to be fully disposed, leading to relatively smaller sizes of SiNPs compared to that calculated through DLS.[7b]

Table S1. Results of ICP-OES analysis

Sample	m_0 (mg)	C_{Si} (mg/L)	wt% Si
SiNPs	198.1±0.1	2774.33	44

The element analysis of SiNPs sample was performed using ICP-OES. First, the initial mass of the SiNPs sample (m_0) was determined after drying. The sample is then dissolved in HNO_3 for ICP-OES analysis. Both Si and any Si-O compounds dissolve well in HNO_3. The ICP-OES analysis yields the concentration of Si (C_{Si}) in the solution, with the value of 2774.33 mg/L. Since the volume (50 mL) of the solution is accurately known in our experiment, the mass of Si atoms in the SiNPs sample are thus able to be calculated as 138.72 mg. The proportion of SiO_2 and Si can then be calculated under the assumption that only these two constituents were present in the original sample mass.[8] Therefore, the mass of Si atoms contained in SiO_2 and Si is readily determined as 51.6 mg and 87.1 mg, respectively, and thus yielding the 44 wt% Si of the SiNPs sample. Note that, since Si are easily oxidized during the treatment process, the exact weight percentage of Si in the SiNPs is actually higher than the above obtained value.

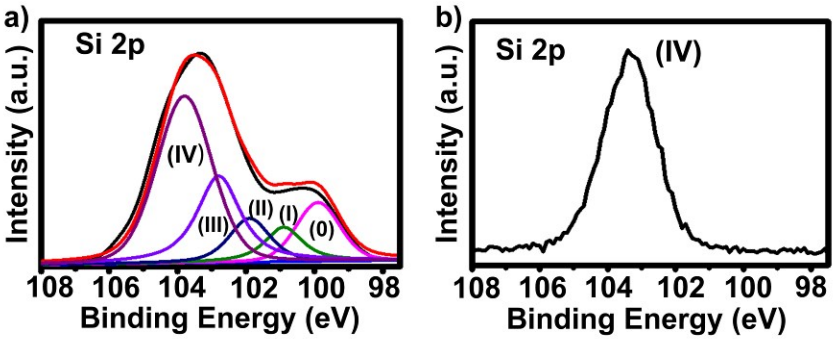

Fig. S6 (a) XPS spectra of SiNPs prepared from rice husks. (b) XPS spectra of rice husks ash (RHA). An intense emission at 99.7 eV ascribed to Si (0) was detected, while other peaks located at 100.9, 101.8, 102.8, and 103.7 eV were attributed to Si suboxides. Accordingly, the ratio value of Si(0)/Si(IV) is determined to be 1:2.80.[9] It is clear from Figure S6 (a) that in addition to the peak corresponding to Si(IV), a distinct peak of around 99.7 eV of binding energy, which is responsible for Si(0), appears in the SiNPs. In contrast, for the RHA sample (Figure S6 (b)), we could not find Si 2p corresponding to Si(0).

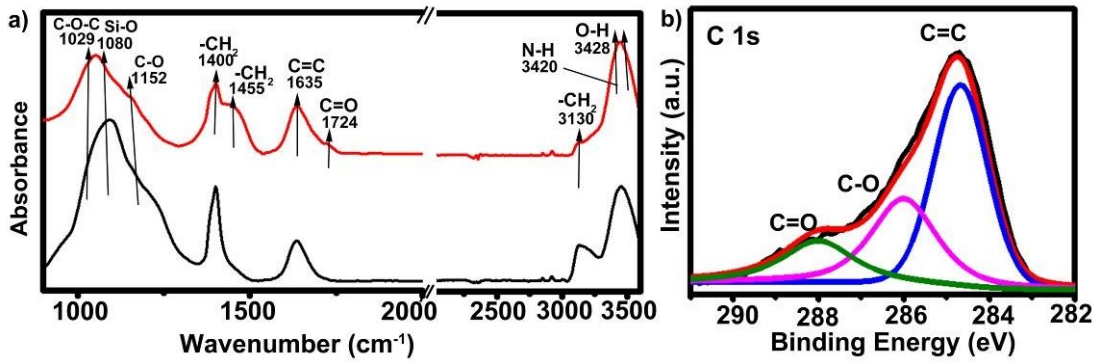

Fig. S7 (a) FTIR spectra of RHA (black line) and SiNPs prepared from RHA (red line). The bands at 3428 cm^{-1} and 3420 cm^{-1} represent the O-H and N-H stretching vibration, respectively. The peaks at 3130 cm^{-1}, 1455 cm^{-1}, 1400 cm^{-1} are assigned to $–CH_2$ groups. The band at 1635 cm^{-1} is assigned due to C=C and C=O stretching, and the band at 1724 cm^{-1} represents the C=O stretching. The absorbance at 1152 cm^{-1}, 1080 cm^{-1}, and 1029 cm^{-1} are, respectively, assigned to the C-O, Si-O and C-O-C bonds.[5,7a,10] (b) High-resolution XPS spectra of C 1s for SiNPs. Fig. S7b shows typical high-resolution C1s spectrum resolved into three different carbon types from the SiNPs surface, which were fitted to 284.7, 286.0 and 288.0 eV, respectively. These three peaks could arise from C=C, C–O, and C=O species, respectively,[11] which is in agreement with the FTIR measurement. These data suggest the origin of the observed fluorescence is partially and possibly produced by the $\sigma^* \rightarrow n$ and $\pi^* \rightarrow \pi$ transitions owing to the C-OH and the aromatic C=C covered on the SiNPs surface.[5] Furthermore, the FTIR and XPS results indicate that the SiNPs contain amino and carboxyl groups, which can be easy to be modified with targeting groups (e.g., goat-antimouse IgG, arginine-glycine-aspartic acid sequence (c(RGDyC)) via established 1-Ethyl-3-(3-dimethylaminopropyl)carbodiimide (EDC)/N-hydroxysuccinimide (NHS) conjugation reaction while maintain their fluorescence property, as well introduced in previous reports.[7a,12]

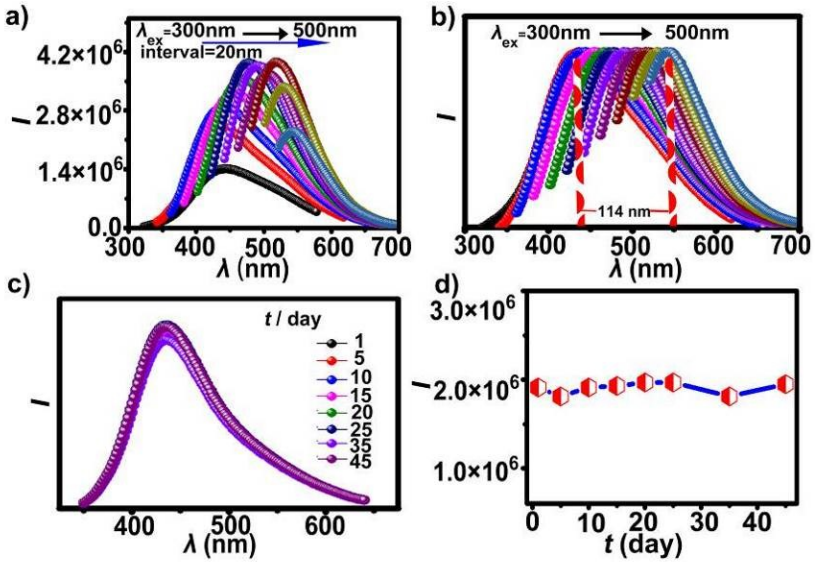

Fig. S8 (a) Excitation-wavelength-dependent emission spectra of SiNPs solution prepared from sugarcane bagasse. The maximum emission wavelength is obviously red-shift from ~430 nm to ~550 nm under serial excitation wavelength from 300 nm to 500 nm. (b) Corresponding normalized PL spectra. (c) Temporal PL spectra (λ_{ex}=330 nm) and (d) corresponding PL intensity of the SiNPs prepared from sugarcane bagasse during 45-day storage in ambient environment without any special protection. The SiNPs prepared from sugarcane bagasse exhibit appreciable excitation-wavelength-dependent fluorescence spectra. The maximum emission peaks shift from ~430 to ~550 nm with the increase of excitation wavelength ranging from 300 to 500 nm. The SiNPs excellent storage stability, retaining stable and strong fluorescence over 1-month storage in ambient conditions.

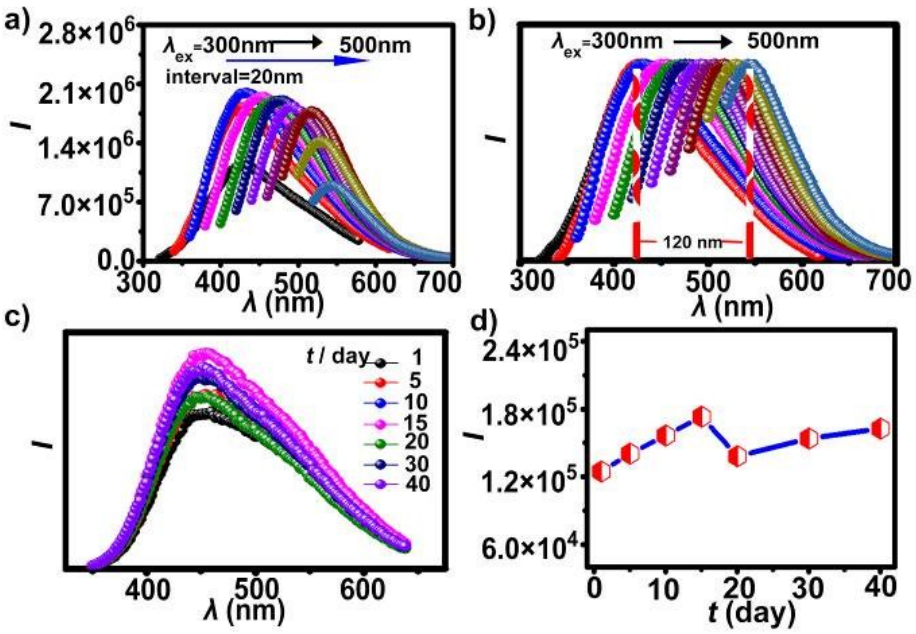

Fig. S9 (a) Excitation-wavelength-dependent emission spectra of SiNPs solution prepared from wheat straw. The maximum emission wavelength is obviously red-shift from ~430 nm to ~550 nm under serial excitation wavelength from 300 nm to 500 nm. (b) Corresponding normalized PL spectra. (c) Temporal PL spectra (λ_{ex}=330 nm) and (d) corresponding PL intensity of the SiNPs prepared from wheat straw during 40-day storage in ambient environment without any special protection. The SiNPs prepared from wheat straw exhibit appreciable excitation-wavelength-dependent fluorescence spectra. The maximum emission peaks shift from ~430 to ~550 nm with the increase of excitation wavelength ranging from 300 to 500 nm. The SiNPs excellent storage stability, retaining stable and strong fluorescence over 1-month storage in ambient conditions.

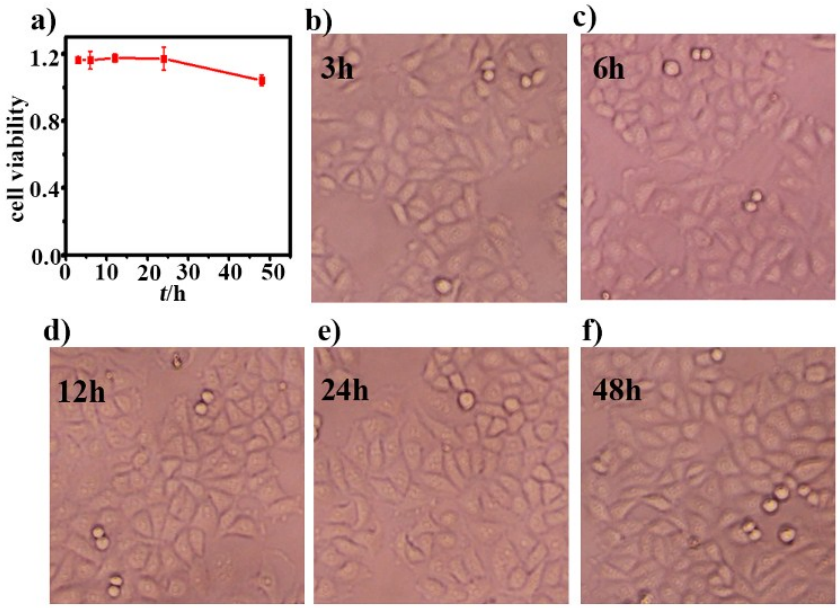

Fig. S10 Cytotoxicity assessment of the SiNPs prepared from RHA. (a) Cell viability of MCF-7 cells incubated with the SiNPs for different time. The cell viability was calculated as a percentage from the viability of the control (untreated) cells. The viability of the control cells was considered 100%. The results are means ± SD from three or four impendent experiments. (b−f) Morphology of MCF-7 cells after incubated with R-SiNPs for 3, 6, 12, 24, and 48 h, respectively. The SiNPs-treated cells preserve >90% cellular viability during 48-h incubation; and meanwhile, no obvious morphological change of MCF7 cells was observed, indicating negligible cytotoxicity of SiNPs.

References

1 X. H. Wang, K. G. Qu, B. L. Xu, J. S. Ren, X. G. Qu, *J. Mater. Chem.,* 2011, **21**, 2445-2450.

2 Y. Y. Su, F. Peng, Z. Y. Jiang, Y. L. Zhong, Y. M. Lu, X. X. Jiang, Q. Huang, C. H. Fan, S. T. Lee, Y. He, *Biomaterials,* 2011, **32**, 5855-5862.

3 (a) M. Patel, A. Karera, P. Prasanna*, J. Mater. Sci.,* 1987, **22**, 2457-2464; (b) L. Y. Sun, *Ind. Eng. Chem. Res.*, 2001, **40***,* 5861-5877; (c) S. Chandrasekhar, K. G. Satyanarayana, P. N. Pramada, P. Raghavan, *J. Mater. Sci.*, 2003, **38,** 3159-3168.

4 N. Liu, K. Huo, M. T. McDowell, J. Zhao, Y. Cui, *Sci. Rep.,* 2013, **3**, 1919.

5 M. Li, S. K. Cushing, X. J. Zhou, S. W. Guo, N. Q. Wu, *J. Mater. Chem.,* 2012, **22**, 23374-23379.

6 (a) S. N. Qu, X. Y. Wang, Q. P. Lu, X. Y. Liu, L. J. Wang, *Angew. Chem.,* 2012, 124, 12381-12384; (b) L. S. K. Pang, J. D. Saxby, S. P. Chatfield, *J. Phys. Chem*., 1993, **97**, 6941-6942; (c) F. J. Hua, M. T. Swihart, E. Ruckenstein, *Langmuir,* 2005, **21**, 6054-6062; (d)Y. S. Jung, K. T. Lee, S. M. Oh, *Electrochimica Acta.,* 2007, **52**, 7061-7067; (e) S. Maher, M. Alsawat, T. Kumeria, D. Fathalla, G. Fetih, A. Santos, F. Habib, D. Losic, *Adv. Funct. Mater.,* 2015, **25**, 5107-5116.

7 (a) Y. L. Zhong, F. Peng, F. Bao, S. Y. Wang, X. Y. Ji, L. Yang, Y. Y. Su, S. T. Lee, Y. He, *J. Am. Chem. Soc.,* 2013, **135**, 8350-8356; (b) Y. He, H. T. Lu, Y. Y. Su, L. M. Sai, Hu, C. H. Fan, L. H. Wang, *Biomaterials,* 2011, **32**, 2133-2140.

8 A. A. Von, L. C. P. M. Smet, D. Munao, A. Evirgen, E. M. Kelder, A. Schmidt-Ott, *J. Nanopart. Res.,* 2011, **13**, 4867-4879.

9 (a) J. J. Romero, M. J. Llansola-Portolés, M. L. Dell'Arciprete, H. B. Rodríguez, A. L. Moore, M. C. Gonzalez, *Chem. Mater.,* 2013, **25**, 3488-3498; (b) K. Furukawa, Y. Liu, H. Nakashima, D. Gao, K. Uchino, K. Muraoka, H. Tsuzuki, *Appl. Phys. Lett.,* 1998, **72**, 725-727.

10 (a) S. C. Wu, Y. L. Zhong, Y. F. Zhou, B. Song, B. B. Chu, X. Y. Ji, Y. Y. Wu, Y. Y. Su, Y. He, *J. Am. Chem. Soc.,* 2015, **137**, 14726-14732; (b) X. Xiao, B. L. Chen, L. Z. Zhu,

Environ. Sci. Technol., 2014, **48**, 3411-3419; (c) B. L. Chen, D. D. Zhou, L. Z. Zhou, *Environ. Sci. Technol.,* 2008, **42**, 5137-5143.

11 (a) B. D. Parka, S. G. Wib, K. H. Leeb, A. P. Singhc, T. H. Yoond, Y. S. Kimb, *Biomass and Bioenergy,* 2004*,* **27,** 353-363; (b) L. P. Xiao, Z. J. Shi, F. Xu, R. C. Sun, *Bioresour. Technol.*, 2012. **118**, 619-623.

12 Song, C. X.; Zhong, Y. L.; Jiang, X. X; Peng, F.; Lu, Y. M.; Ji X. Y., Su, Y. Y.; He, Y. *Anal. Chem.,* 2015, **87**, 6718-6723.